

**INHIBITION OF THE NUCLEAR EXPORT RECEPTOR XPO1
AS A THERAPEUTIC TARGET FOR PLATINUM RESISTANT OVARIAN CANCER**

Ying Chen¹, Sandra Catalina Camacho¹, Thomas R. Silvers¹, Albiruni RA Razak², Nashat Y Gabrail³, John F Gerecitano⁴, Eva Kalir¹, Elena Pereira⁵, Brad R. Evans¹, Susan J. Ramus⁶, Fei Huang¹, Nolan Priedigkeit¹, Estefania Rodriguez¹, Michael Donovan⁷, Faisal Khan⁷, Tamara Kalir⁷, Robert Sebra¹, Andrew Uzilov¹, Rong Chen¹, Rileen Sinha¹, Richard Halpert⁸, Jean-Noel Billaud⁸, Sharon Shacham⁹, Dilara McCauley⁹, Yosef Landesman⁹, Tami Rashal⁹, Michael Kauffman⁹, Mansoor R. Mirza⁹, Morten Mau-Sørensen¹⁰, Peter Dottino⁵, John A. Martignetti^{1,5,11}

¹ Genetics & Genomic Sciences, Icahn School of Medicine at Mount Sinai, New York, NY. ²Drug Development Program, Princess Margaret Cancer Center, Toronto, Canada. ³ Gabrail Cancer Center, Canton, OH, USA. ⁴Memorial Sloan Kettering Cancer Center, New York, NY, USA. ⁵Obstetrics, Gynecology and Reproductive Science, Icahn School of Medicine at Mount Sinai, New York, NY. ⁶ School of Women's and Children's Health, University of New South Wales, Australia. ⁷Department of Pathology, Icahn School of Medicine at Mount Sinai, New York, NY. ⁸Qiagen, Redwood City, CA, USA, ⁹Karyopharm Therapeutics Inc, Natick, MA, USA, ¹⁰Department of Oncology, Rigshospitalet, Copenhagen, Denmark, ¹¹Western Connecticut Health Network, Danbury, CT.

Key words: Ovarian Cancer, XPO1, platinum resistance

Corresponding author: John A. Martignetti, 1425 Madison Ave, Room 14-26, New York, NY, 10029. Tel: 212-659-6744, Fax: 212-360-1809. email: john.martignetti@gmail.com

Disclosure of Potential Conflicts of Interest

Sharon Shacham, Dilara McCauley, Yosef Landesman, Tami Rashal, Michael Kauffman, and Mansoor R. Mirza are employees of Karyopharm Therapeutics, Inc and produce two of the compounds, KPT-185 and KPT-330, described in this manuscript. No potential conflicts of interest were disclosed by the other authors.

Manuscript includes 5000 words of text and 6 figures/tables.

ABSTRACT

Purpose: Ovarian cancer's (OvCa) high fatality-to-case ratio is directly related to platinum resistance. Exportin-1 (XPO1) is a nuclear exporter that mediates nuclear export of multiple tumor suppressors. We investigated possible clinicopathologic correlations of XPO1 expression levels and evaluated the efficacy of XPO1 inhibition as a therapeutic strategy in platinum sensitive and resistant OvCa.

Experimental design: XPO1 expression levels were analyzed to define clinicopathologic correlates using both TCGA/GEO data sets and tissue microarrays (TMAs). The effect of XPO1 inhibition, using the small molecule inhibitors KPT-185 and KPT-330 (selinexor), alone or in combination with a platinum agent on cell viability, apoptosis, and the transcriptome was tested in immortalized and patient-derived OvCa cell lines (PDCL) and platinum-resistant mice (PDX). Seven patients with late-stage, recurrent, and heavily pretreated OvCa were treated with an oral XPO1 inhibitor.

Results: XPO1 RNA overexpression and protein nuclear localization were correlated with decreased survival and platinum resistance in OvCa. Targeted XPO1 inhibition decreased cell viability and synergistically restored platinum sensitivity in both immortalized OvCa cells and PDCL. The XPO1 inhibitor-mediated apoptosis occurred through both p53-dependent and p53-independent signaling pathways. Selinexor treatment, alone and in combination with platinum, markedly decreased tumor growth and prolonged survival in platinum-resistant PDX and mice. In selinexor-treated patients, tumor growth was halted in three of five patients, including one with a partial response and was safely-tolerated by all.

Conclusion: Taken together these results provide evidence that XPO1 inhibition represents a new therapeutic strategy for overcoming platinum resistance in women with OvCa.

Translational relevance statement: Ovarian cancer is the most lethal female reproductive tract malignancy worldwide. While the majority of patients appear to respond to first-line platinum-based chemotherapy, in reality, the majority of these women will suffer a recurrence of chemoresistant disease, having a five-year survival of only ~ 30%. Here we show that overexpression of the nuclear exporter protein XPO1 correlates with worse survival and platinum resistance. Targeted inhibition of XPO1, using the small molecule XPO1 inhibitors KPT-185 and KPT-330, results in apoptosis and synergistic cell death when used in combination with platinum even in platinum resistant ovarian cancer cell lines and PDX mice. Patients with late-stage, recurrent and heavily pretreated ovarian cancer were treated with single agent KPT-330. Tumor growth was halted in three of five patients, including one with

a partial response. Together these results provide evidence for XPO1 inhibition as a novel paradigm in overcoming platinum resistance in OvCa.

INTRODUCTION

Ovarian cancer (OvCa) is the most lethal reproductive tract malignancy in the US, with over 22,000 cases and approximately 16,000 deaths annually (1). OvCa's high fatality-to-case ratio is directly related to the fact that most patients will develop resistance to platinum chemotherapy and eventually will die from their disease (2). New therapeutic targets and/or treatments restoring platinum sensitivity are urgently needed.

Nuclear-cytoplasmic transport plays a crucial role in maintaining normal cellular function (3), and defects in this process are increasingly identified in solid and hematologic cancers (4,5). One of the key nuclear transport proteins is exportin 1 (6)(XPO1; also known as chromosomal regional maintenance 1, CRM1 (Supplementary Figure 1)). XPO1, one of eight known nuclear exporters, regulates the nuclear-cytoplasmic partitioning of a number of nuclear export sequence (NES) containing tumor suppressors, cell cycle inhibitors and oncogenes (7-9). XPO1 overexpression has been suggested to be a general feature of cellular transformation (9) and has been observed in a number of hematologic and solid tumors (9-13) including OvCA (10). Most relevant to this study, XPO1 is the only known transporter for a number of well-characterized OvCa-associated proteins, including p53 (11-12), BRCA1(13), I κ B α (14), KLF6 (15), sequestosome 1 (SQSTM1; also known as p62) and PP2A (CIP2A) (16), all of which play roles in OvCa initiation, cell cycle progression, the DNA damage response, apoptosis, autophagy, and chemoresistance. Therefore, XPO1 seems an excellent OvCA therapeutic target.

Targeted inhibition of XPO1 with leptomycin B (LMB), a naturally occurring XPO1 inhibitor isolated from *Streptomyces* bacteria, yields antitumor responses in a number of different hematologic and solid tumor models, but within a very narrow therapeutic index (9, 17, 18). Unfortunately, LMB's off-target effects render it inappropriate for therapeutic use (17, 19). Given these constraints and therapeutic potential, a number of different classes of Selective Inhibitors of Nuclear Export (SINE) have been synthesized and are being evaluated for therapeutic efficacy (4, 5, 20). KPT-185 and KPT-330 (generic name: selinexor) represent two SINE compounds that potently, selectively, and covalently inhibit XPO1. Although these molecules bind to the same reactive Cys528 residue that LMB binds (17, 21), they do so in a slowly reversible fashion (21), improving their selectivity and reducing their off-target effects (22, 23). An ester moiety on KPT-185 precludes its oral bioavailability and conscripts it to *in vitro* use (21), while an amide moiety on KPT-330 is associated with excellent bioavailability in all species tested. Both SINE compounds have demonstrated antitumor activity in a number of different

cancer types (22-28).

Herein, we characterize the anti-tumor efficacy of SINE compound-mediated XPO1 inhibition as well as the efficacy of these agents in the context of OvCa. These agents decreased OvCa proliferation and tumor growth, acted synergistically with cisplatin (a platinum-based chemotherapeutic agent) to induce apoptosis, and increased survival in two complementary OvCa mouse models. Moreover, the results of oral XPO1 inhibition in heavily pretreated patients with platinum-resistant / refractory OvCa patients demonstrated the safety, tolerability, and efficacy of the XPO1 inhibitor selinexor. Our study therefore provides the rationale for the therapeutic strategy of targeting a critical protein in the nuclear transport receptor complex in platinum-resistant OvCa.

MATERIALS AND METHODS

Patients, specimen collection and patient-derived cell lines.

OvCa tumor samples were collected, with patient consent, at the time of surgery at a single institution under an IRB-approved protocol. Following examination in Pathology for confirmation and staging, tumor tissue sections were generated and used for establishing patient-derived cell lines and generating xenograft mouse models. Patient-derived cell lines were established based upon a previously published protocol (29).

Tissue microarray and immunofluorescence

Tissue microarrays (TMAs) were constructed from 56 pathologist selected, 1.0 mm tumor cores of formalin-fixed, paraffin-embedded (FFPE) OvCa specimens (Beecher Instrument, Sun Prairie, Wisconsin) in triplicate. All were patient samples of the Mount Sinai Hospital. 83% of the samples were serous OvCa, and all of these were defined as high grade (grades 2 and 3). In brief, TMA sections were immunostained with the XPO1 antibody SC-5595 (Santa Cruz Biotechnology) using the Benchmark XT (Ventana/Roche, Oro Valley, AZ) with the ultraVIEW Universal DAB Detection Kit (Ventana/Roche). Isotype rabbit IgG1 was used as a negative control. The intensity of the XPO1 immunostaining in tumor cells was evaluated independently and then overseen by a senior pathologist (M.D.). All readers were blinded to patient outcomes. Intensity, percent positivity and cellular localization (i.e. nuclear and cytoplasm) were analyzed for each core, with a calculated H-score (% positivity (0-100) multiplied by intensity (1-3+), maximum 300) determined for each. Cut-points were derived based on maximizing sensitivity and specificity for predicting the outcomes. FFPE OVCAR3 cells were used as a positive control.

Normal ovary, fallopian tube and endometrial tissues, incorporated into the arrays, were evaluated as negative tissue controls along with whole sections of normal colon tissue, normal testis and normal lung during XPO1 development assays.

For immunofluorescence studies, cells were first plated on coverslips. At designated time points, cells were fixed with 4% paraformaldehyde and permeabilized on ice with 0.5% Triton X-100 (Sigma, St. Louis, MO) or 90% methanol for 10 minutes. After incubation with primary and secondary antibodies, cells were counterstained with DAPI and mounted with Vectashield (Vector Lab, Burlingame, CA). Images were acquired and analyzed using the Axion plan software on a Zeiss Axion microscope (Zeiss, Oberkochen, Germany).

Antibodies

Anti-XPO1 (H-300), anti-p53 (DO-1), anti-lamin A/C (N-18), anti-GAPDH, and anti-NF- κ B p65 were obtained from Santa Cruz Biotechnology (Santa Cruz, CA). Anti-cleaved caspases-8 (Asp391), -9 (Asp330), and -3 (Asp175), anti-cleaved-PARP (Asp214), anti-phospho-p53 (Ser15), anti-Erk1/2, anti-phospho-p44/42 Erk1/2 (Thr202/Tyr204), anti-Bcl-xL, anti-I κ B α , anti-phospho-p65 (Ser536), and anti-clAP1/2 were obtained from Cell Signaling Technology (Danvers, MA).

Cell culture and reagents

The OvCa cell lines A2780, CP70, OVCAR3, and SKOV3 were purchased from ATCC (Manassas, VA) and cultured in DMEM medium supplemented with 10% FBS. Immortalized human normal fallopian tube epithelial cell line FT33-shp53-R24C was purchased from Applied Biological Materials Inc (ABM, Richmond, Canada) and cultured in Prigrow IV Medium with 10% FBS in PriCoat™ T25 Flasks (ABM). Human fibroblast cell lines IMR-90, Wi-38 were purchased from ATCC and cultured in MEM medium with 10% FBS. Human fibroblast cell lines AG060062 and GM17071A were maintained in our lab (30). KPT-185 and KPT-330 were provided by Karyopharm Therapeutics (Newton, MA). DMSO was used as the diluent control for all *in vitro* studies. All cell-based experiments were repeated a minimum of three times.

MTT assay and evaluation of drug interaction

The cell proliferation reagent 3-(4,5-Dimethylthiazol-2-yl)-2,5-diphenyltetrazolium bromide (MTT) was used to evaluate cell viability. Viability was measured using the following formula: relative viability = (experimental absorbance-background absorbance) / (untreated controls absorbance-

background absorbance) $\times 100\%$. The IC50 values of cisplatin and KPT-185 at which the proliferation was reduced by 50% compared with the untreated control were calculated using nonlinear regression (GraphPad Prism v3.0, GraphPad software, San Diego, CA). Drug synergy analysis was performed using Chou-Talalay's isobolographic method (31) and combination index (CI) was calculated using Calcosyn software suite (Biosoft, Cambridge, UK). If $CI < 1$, the drugs act synergistically; if $CI =$ or > 1 , the drugs interaction is defined as additive or antagonistic, respectively.

OvCa mouse models

All animal studies were conducted in accordance with the rules and regulations of the Institutional Animal Care and Use Committee (IACUC) at the Icahn School of Medicine at Mount Sinai. For these models, 6-week-old female Rag1 knockout mice (C.129S7(B6)-Rag1^{tm1Mom}/J) and Balb/c nude mice were purchased from Jackson Laboratories (Bar Harbor, ME).

Patient-derived ovarian cancer xenograft mouse models (PDX). OvCa tissue collected at the time of surgery was minced into pieces approximately $\sim 1.5 \text{ mm}^3$ in size and implanted into the flanks of Rag1^{-/-} mice. Once tumors developed in mice, a representative section from each cohort was harvested and sent for pathology review. Paired genomic DNA was isolated from the patient's original tumor and the mouse xenotransplant and p53 and BRCA genes were sequenced using a custom targeted gene panel (Ion Torrent, Life Technology, Grand Island, NY).

When PDX tumor volume ($V = L \times W^2 \times 0.5$, L = longest diameter, W = shortest diameter) reached $\sim 125 \text{ mm}^3$, KPT-330 (10mg/kg) was delivered three times per week via oral gavage. Mice with tumors $> 1000 \text{ mm}^3$ were euthanized as per IACUC regulations. All mice were observed until 120 days after treatment, at which time the experiments were terminated.

CP70 mouse model (CP70-OvCaX). 1×10^6 luciferase-expressing CP70 cells were injected IP into nude mice. One week post tumor cell injection, tumor engraftment was confirmed by bioluminescence (BLI) using the IVIS Spectrum Pre-clinical In Vivo Imaging System (PerkinElmer, Waltham, MA), as we have previously described (32). Tumor-bearing mice were randomly assigned to four different treatment regimens: vehicle control, cisplatin alone (2.5mg/kg, twice/week), KPT-330 alone (15mg/kg, twice/week), and combination treatment with cisplatin and KPT-330. Tumor growth was monitored twice/week. For all tumor tissues harvested, paraffin sections were prepared for IHC staining and TUNEL assay.

Phase I clinical trial

A multi-center phase I clinical trial was performed to assess the safety, tolerability, and efficacy of Selinexor (KPT-330) in late-stage, platinum-resistant OvCa patients. Approval was obtained from the respective Institutional Review Boards at participating sites. Patients were eligible for study participation if they met the following criteria: 18 years of age or older, had OvCa resistant or refractory to standard therapy, an Eastern Cooperative Oncology Group performance status (ECOG PS) <2, and measurable disease by Response Evaluation Criteria in Solid Tumors version 1.1 (RECIST 1.1). Additionally, adequate renal, hepatic and hematologic functions were required. Patients received single agent treatment with 30–35mg/m² oral KPT-330 2-3 times weekly (8-10 doses/4-week cycle). Response was evaluated every 2 cycles (RECIST 1.1). Dose-limiting toxicity was defined as events occurring in the first 28 days at the target dose. These events included: severe nausea/vomiting/diarrhea and fatigue lasting > 5 days, hematological toxicities, and liver/renal function abnormalities. Treatment could be discontinued in the event of dose-limiting toxicities, and dose modifications secondary to toxicities were not allowed. Information regarding the statistical design of the overall phase I study is available (33).

Statistical analysis

Significant differences between groups were determined using the Student's *t* test. Survival data analysis was performed using the Kaplan-Meier and log-rank tests (GraphPad Prism software v5.0).

RESULTS

XPO1 overexpression and nuclear localization are correlated with decreased survival and platinum resistance.

In seeking to gain an understanding of the potential value of XPO1 as a therapeutic target in OvCa, we first analyzed *in silico* the correlation between XPO1 RNA expression levels and progression free survival (PFS) and overall survival (OS) in OvCa using the largest independent, multi-center high-grade OvCa sample dataset available. Using the cBIO Cancer Genomics Portal (34) we interrogated all 489 cases analyzed by Agilent expression chips and the 261 cases that have associated RNASeq data. With an overexpression cutoff of 1.2 standard deviations (SDs) above the mean, *XPO1* was found to be overexpressed in 24% of the Agilent

data cases and in 27% of the RNASeq data cases. Across all of the RNASeq data, *XPO1* overexpression was associated both with worse OS ($p=0.029$) and PFS ($p=0.01$; Supplementary Table 1).

We next used Kaplan-Meier Plotter (35) to further explore the association between *XPO1* overexpression and survival using Gene Expression Omnibus (GEO) and TCGA datasets. Again we focused exclusively on high grade serous OvCa and included only those individuals treated with a platinum agent since platinum agents are the gold-standard treatment for primary disease. Because surgical debulking status remains one of the most significant contributors to overall survival (36), we first analyzed all patients together regardless of debulking status and then independently examined those with optimal and suboptimal (defined as >1 cm of residual tumor following surgery) debulking following surgery). An association with overall survival was present in patients regardless of their debulking status ($p=0.048$). In suboptimally debulked patients, *XPO1* overexpression was associated both with worse PFS ($p=0.048$; HR=1.45, 95% CI 1.0-2.1) and OS ($p=0.0213$; HR=1.57, 95% CI 1.07-2.31, Fig. 1a, left and right, respectively). We furthermore limited our analysis to the subset of patients with suboptimal surgical debulking defined as >1 cm of residual tumor following surgery. In these patients, *XPO1* overexpression was associated both with worse PFS ($p=0.048$; HR=1.45, 95% CI 1.0-2.1) and OS ($p=0.0213$; HR=1.57, 95% CI 1.07-2.31, Fig. 1a, left and right, respectively).

We next directly quantified *XPO1* protein levels and subcellular localization to complement the RNA-based, *in silico* analyses. First, we examined *XPO1* expression in four well characterized and frequently studied immortalized OvCa cell lines (A2780, CP70, OVCAR3, and SKOV3) and compared these expression levels to other ovarian- and non-ovarian-derived cell lines. Western blot analysis demonstrated consistently higher levels of *XPO1* expression in the four OvCa cell lines compared to non-cancerous ovarian surface epithelial cells (IOSE527), a fallopian tube cell line (FT33-shp53-R24C) and four fibroblast cell lines (IMR-90, Wi-38, AG060062 and GM17071A) (Fig. 1b).

Finally, we quantitated and localized *XPO1* protein levels *in situ* across a wide range of patient-derived OvCa tissues using a tissue microarray (TMA) representing patient samples from individuals treated at our institution. We analyzed samples from 56 patients with high grade serous OvCa representing 143 evaluable cores (Supplementary Table 2). Nuclear and cytoplasmic staining were analyzed independently. *XPO1* expression levels ranged from low

(30%, 1+ cytoplasmic staining; left panel) to high (90%, 3+ nuclear and cytoplasmic; right panel) across the sample set (Fig. 1c). Clinically-relevant clinicopathologic associations were identified (37) based on XPO1 expression levels and nuclear vs. cytoplasmic distribution. Increased nuclear XPO1 expression correlated with shorter 5-year PFS (concordance index of 0.40, HR 2.0, cut-point 90, $p < 0.003$; Figure 1d) and with platinum resistance (score = 0.227; scale of -1 to +1). A correlation with overall survival was also present but was weaker (concordance index of 0.44; not shown). Conversely, XPO1 cytoplasmic staining was positively correlated (score 0.262; scale of -1 to +1) with those patients who were survivors including those who were with no evidence of disease (NED) and alive-with-disease (AWD). There was a statistically significant difference in cytoplasmic expression in cancer survivors versus those who had died of their disease (p -value = 0.0042).

KPT-185 selectively inhibits proliferation and induces apoptosis even in platinum-resistant OvCa cells

Having established these associations, we next investigated the anticancer efficacy of XPO1 inhibition, particularly in the context of platinum resistance. We first examined the effects of the XPO1 inhibitor KPT-185 on cisplatin-sensitive A2780 cells, A2780-derived cisplatin-resistant CP70 cells (38), and cisplatin-resistant OVCAR3 (39) and SKOV3 (40) cells. Submicromolar KPT-185 concentrations significantly inhibited growth of all cell lines (Fig. 2a). The IC₅₀s in these cell lines ranged from 46.53 nM to 328.7 nM. Selinexor, with a similar molecular weight as KPT-185, achieves serum levels $>1.5\mu\text{M}$ at doses below the maximum tolerated dose in patients with cancer, indicating that these concentrations are clinically relevant. In marked contrast, and highlighting a specificity for the cancer-derived cell lines, a KPT-185 concentration of 4000 nM failed to kill non-cancerous IOSE527 cells and concentrations greater than 10,000 nM had not demonstrable toxic effect on the other non-cancerous cell lines tested (Fig. 2a). We further corroborated this finding of an increased cancer cell sensitivity by testing the effect of KPT-185 on patient-derived primary tumor cells versus patient-derived benign cells. Forty-four patient-derived high grade serous OvCA cell lines and 6 patient-derived benign ovarian cell lines were tested. While the HGSOC-derived cell lines had an average IC₅₀ of 3.2 μM , the average IC₅₀ for the benign cell lines (19.1 μM) was nearly six times greater ($p < 0.001$) (Supplementary Fig. 2). Taken together, these findings in both the immortalized and patient-derived cell lines are in accord with previous findings that 40 μM of KPT-185 or related SINEs are not toxic to normal lymphocytes, bone marrow cells, primary hepatocytes, and other normal cells (25,26). Finally, and given that many of the commonly used OvCa cell lines do not share

the same genetic profiles of native tumors, most notably that unlike tumors, the cell lines are TP53 wild type, we also investigated the efficacy of KPT-185 in patient-derived primary OvCa cell lines. In addition to testing the efficacy of KPT-185 in the above forty-four patient-derived cells, primary tumor cell lines derived from 17 different OvCa patients with either primary or recurrent disease and platinum sensitive and resistant tumors (Supplementary Table 3) were treated with KPT-185. Regardless of platinum or other chemotherapy resistance status, all patient-derived OvCa cell lines were significantly growth inhibited by KPT-185 (Fig. 2f, red line).

To determine the mechanism of KPT-185-mediated decrease in cell viability, we first determined the degree of cell cycle arrest in each cell line. While KPT-185 treatment resulted in G1 phase arrest in A2780 cells ($p = 0.006$) no significant degree of arrest was noted for CP70, OVCAR3, or SKOV3 cells (Supplementary Fig. 3). In these latter three cell lines, we next quantitated the degree of apoptosis induction. All three cell lines initiated apoptosis following KPT-185 treatment and apoptosis could be almost completely blocked by the use of the anti-apoptotic agent Z-VAD-FMK (Fig. 2b). KPT-185 treatment resulted in marked increases in caspases 3, 8, and 9, as well as PARP cleavage (Fig. 2c), suggesting activation of the apoptotic cascade through both the intrinsic and extrinsic pathways.

KPT-185 acts synergistically with platinum to increase chemosensitivity independent of cellular p53 status

Because platinum resistance is the foremost obstacle to long-term successful OvCa treatment, we explored the effect of combining SINEs and cisplatin. While the well-studied isogenic OvCa lines A2780 and CP70 were originally derived to study cisplatin resistance differences, they are both p53 WT. By contrast, nearly 100% of late-stage serous OvCa tumors are deficient for p53 or possess a mutated p53 (41). Thus, for clinical relevance, SINE compounds must be effective even in p53 mutated/deficient tumor cells. We determined the effect of increasing concentrations of cisplatin alone or in combination with KPT-185 on cell viability in the four immortalized OvCa cell lines and also the set of patient-derived OvCa cell lines, which were established from both platinum sensitive and resistant tumors, as described above.

Regardless of p53 status, KPT-185 enhanced the efficacy of cisplatin in all cell lines (Fig. 2d, e, and f). In cisplatin resistant CP70 cells, combinatorial treatment resulted in an IC₅₀ similar to that of the isogenic cisplatin sensitive parent line (A2780), indicating an increase in platinum sensitivity (Fig. 2d, e). The combination index (CI) was calculated to determine the degree of

synergy. KPT-185 and cisplatin were shown to be synergistic as demonstrated by their low CI values at all concentrations explored (Supplementary Fig. 4). Isobologram analysis revealed that the combination of drugs was consistent with a synergistic, not simply additive effect. The CI in the immortalized cell lines ranged from 0.51 to 0.69.

Synergy between KPT-185 and cisplatin was also demonstrated in all the patient-derived cell lines that were tested (Fig. 2f). Even doses as low as 500 nM of KPT-185, an average IC₂₅ dose, effectively lowered cisplatin IC₅₀ levels, on average, > 4-fold (13.53 μ M vs. 3.15 μ M; Fig. 2f). The combined CI value was 0.55, indicating synergy between these two drugs.

SINE compounds induce apoptosis through p53-dependent and independent pathways

As described above, KPT-185 effectively induced apoptosis in all the OvCa cell lines tested regardless of their p53 status. This together with the role of p53 in apoptosis and as a recognized XPO1 cargo protein (7) led us to explore whether the mechanisms of SINE-induced apoptosis could be mediated through both p53-dependent and independent pathways.

We first examined the effect of KPT-185 treatment on the p53 wild type (WT) CP70 cell line. p53 nuclear accumulation and up-regulated expression were readily apparent following KPT-185 treatment (Fig. 3a left panel, 3b). Increased phospho-p53 (Ser15) expression was confirmed via Western blot (Fig. 3c). Previous studies have demonstrated that the Ras-Raf-ERK signaling cascade functionally interacts with p53 activation in apoptosis (42); therefore, we also investigated the degree, if any, of ERK1/2 activation. Following KPT-185 treatment phosphorylated ERK1/2 levels increased in the nucleus (Fig. 3c). The use of the highly selective p53 inhibitor Pifithrin-alpha (PFT- α) (27) suppressed phosphorylated-ERK1/2 expression (Fig. 3c), consistently increased Bcl-xL expression (Fig. 3c, lower panel), and decreased apoptosis (Fig. 3d). We also examined the effect of targeted p53 knockdown using siRNA. CP70 cells were transfected with either p53 siRNA or control scrambled siRNA (scRNA) and cells treated with KPT-185 (Supplementary Fig. 5). The effect of p53 loss on apoptosis was then measured by FACS analysis. While treatment with KPT-185 in a p53 WT background resulted in >25% apoptosis, silencing p53 markedly blocked this response such that cell death was essentially at the background levels observed in the control cells. Together, these findings provide evidence for p53-dependant SINE-mediated ERK1/2 activation, suggesting that in CP70 cells, ERK1/2 is a downstream regulator of p53 during KPT-185-mediated apoptosis.

As an independent method to confirm the role of p53 in the response of CP70 cells to KPT-185, and do so in an agnostic manner, we performed a whole-genome RNA analysis. CP70 cells treated with KPT-185 were compared to sham-treated cells and total RNA isolated and interrogated by microarray (Illumina, HumanHT12, v4 Expression BeadChip). The Upstream Regulator Analysis (URA) of Ingenuity Pathway Analysis (IPA) was used to identify the predicted state (activation / inhibition) and cascade of upstream transcriptional regulators that could explain observed gene expression changes following KPT-185 treatment. In total, more than 20 activated pathways were identified. The most activated pathway in this analysis was p53. The activation Z-score was 3.5, and p value, 1.67E-05. The p53 network (i.e. p53 downstream targets) and its direction of activation are shown in Supplementary Fig. 6.

By contrast, we hypothesized that during p53-independent apoptosis, in OvCa cells with inactive or mutated p53, KPT-185's pro-apoptotic effect could be mediated by an alteration of the NF- κ B pro-survival pathway. This was based on the complementary findings that: (1) NF- κ B suppresses programmed cell death and promotes tumor growth (43), (2) NF- κ B activity can be downregulated by XPO1 inhibition in mantle cell lymphoma (23), and (3) NF- κ B has been linked to OvCa (44). In untreated SKOV3 and OVCAR3 cells, NF- κ B p65 and I κ B α were abundantly expressed in the cytoplasm. KPT-185 treatment altered this subcellular localization such that nuclear accumulation of I κ B α and p65 was readily apparent (Fig. 4a, b) with concomitant slight decreases of their cytoplasmic expression. As an indication of suppressed NF- κ B activity, KPT-185 treatment reduced phosphorylated p65 levels with decreased expression of p65-target genes cIAP1 and cIAP2 (Fig. 4c).

Since KPT-185 induced nuclear translocation of both p65 and I κ B α and this correlated with decreased NF- κ B activity, we asked whether this inhibition was the result of I κ B α directly binding p65 in the nucleus. In support of this translocation-based mechanism, I κ B α bound NF κ B only in immunoprecipitates from the nuclear fractions of KPT-185 treated cells (Fig. 4d). Loss of I κ B α , through siRNA-mediated silencing, reversed the suppression of p65 activity (Fig. 4e), increased cIAP1 and cIAP2 expression (Fig. 4e) and decreased apoptosis (Fig. 4f). Thus, these results indicated that this p53-independent apoptosis induced by KPT-185 is mediated by increased nuclear levels of I κ B α .

XPO1 inhibition increases platinum sensitivity and survival in OvCa-bearing mice

We assessed the *in vivo* anti-tumor efficacy of SINE compound KPT-330 using two complementary OvCa mouse models. First, we tested an intraperitoneal (ip) model of OvCa growth and dissemination using cisplatin-resistant CP70 cells. Seventy tumor-bearing mice were divided into four groups: vehicle control (n=16), cisplatin treated (n=17), KPT-330 treated (n=16), and combination cisplatin/KPT-330 treated (n=21). We confirmed the highly chemoresistant nature of the CP70 cell line by demonstrating a slight (four day) increase in median survival among cisplatin-treated mice compared to control mice (Fig. 5a, $p < 0.0005$). However, oral (gavage) selinexor treatment significantly increased the median survival compared to control (32d versus 24d, $p < 0.0001$) and cisplatin-treated (32d versus 28d, $p < 0.005$; Figure 5a) mice. The greatest survival benefit was achieved with the selinexor-cisplatin combination, which had a median survival of 37 days – a ~30% increase in survival compared to cisplatin alone ($p < 0.0001$) and a ~15% increase in survival compared to selinexor alone ($p = 0.01$). More than 60% (13/21) and ~30% of co-treated mice survived beyond the maximum survival date of the cisplatin only (31 days) and selinexor only treated (43 days) mice, respectively. Immunohistochemical staining of *ex vivo* tumor samples following treatment is shown (Fig. 5b).

We next assessed the anti-tumor efficacy of oral selinexor on OvCa xenograft (PDX) mice. The PDX OvCa model has recently been reported to maintain histologic, genomic, and, importantly, platinum-treatment response profiles similar to those of the donor OvCa tumor (45). Our PDX mice were derived from seven independent patients with high grade serous OvCa. Each patient had received a minimum of six rounds of chemotherapy, and at least five of them multiple drugs including platinum, taxol and bevacizumab. Five patients had recurrent disease and failed cisplatin treatment, and one each had cisplatin sensitive or resistant primary tumors (Supplementary Fig. 7). Our PDX models maintained the histologic features of the original donor tumor (upper panel), and, as demonstrated by directed DNA sequencing of the human/murine tumor pairs and the patient's germline DNA, also maintained their p53 and BRCA mutation profiles (lower panel).

Within one to five months after tumor tissue implantation, tumors developed in each of the mice. Selinexor-treated mice experienced significant and prolonged tumor regression, which was in marked contrast to controls ($P < 0.0001$, Fig. 5c, upper panel). Dramatic tumor shrinkage (average volume reduction $\geq 99\%$) was observed in nearly 90% (19/22) of selinexor treated

mice. Their tumors were undetectable or only barely evident, even with open exploration of the inoculation site (Fig. 5d). For the three mice without tumor shrinkage, tumor growth was nonetheless markedly delayed. As expected, tumor volume decreases were accompanied by survival increases. Most strikingly, no control mice survived beyond 38 days (median survival, 22.5 days); however, all KPT-330 treated mice with tumor shrinkage survived the pre-defined 120-day window of this experiment (Fig. 5c, lower panel).

To directly ascertain whether selinexor restores cisplatin sensitivity *in vivo*, we selected a PDX model generated from a recurrent, cisplatin-resistant patient tumor (PT171, p53 mutated) for more in-depth analysis. The same four different treatment groups, vehicle control (n=2), cisplatin alone (n=2), KPT-330 alone (n=3), and combination cisplatin/KPT-330 (n=2), were compared. Although cisplatin delayed tumor growth ($p < 0.001$, Fig. 5e), tumor volumes nonetheless increased 4-fold within 40 days. By contrast, selinexor treatment, either alone or in combination with cisplatin, significantly decreased tumor volume (Fig. 5e insert, $p < 0.0005$). Tumor volume decreased by more than 90% in selinexor treated mice, with more rapid initial decreases in tumor volume observed in KPT-330-cisplatin treated mice. Additionally, no evidence of tumors remained by day 50 in selinexor-cisplatin treated mice, even upon *ex vivo* inspection. As expected, selinexor treatment significantly prolonged survival, with control and cisplatin treated mice dying within 20 and 30 days, respectively, but with selinexor-cisplatin treated mice surviving beyond the pre-defined cutoff of 120 days.

Selinexor is safely tolerated by OvCa patients and can decrease tumor volume

Based in part upon these results, a phase I, single-agent clinical trial (ClinicalTrials.gov: NCT01607905) was initiated to determine the safety, tolerability, and efficacy of selinexor in solid tumor patients. This trial included seven patients with heavily pretreated, relapsed OvCa refractory to platinum (Fig. 6a). Patients received 30–35 mg/m² of oral selinexor (the maximum tolerated dose) (33). The most common adverse events were fatigue, nausea, anorexia, diarrhea, and vomiting, which were managed with supportive care (Fig. 6b). No adverse events required discontinuation of treatment. There were no major organ toxicities and no life threatening or grade 4 adverse events were reported. Pharmacokinetics achieved in patients was comparable to those observed in mice. Selinexor resulted in up to a 10-fold induction of XPO1 mRNA measured by qRT-PCR in patient-leukocytes. In selected solid tumors, p53 and I κ B α nuclear accumulation and induction of apoptosis were confirmed in repeated tumor biopsies after 3-4 weeks of selinexor treatment.

Two patients withdrew for non-drug-related issues. Of the five evaluable patients, selinexor inhibited tumor growth in three (Fig. 6c, d). One (patient #043-815; days on study=156) experienced a partial response whereas disease stabilized in two (patient #043-047, days on study=115 with maximal CA-125 reduction 39%; patient #043-046, days on study 400 days with maximal CA-125 reduction 75%). The CA-125 levels over time are presented in Figure 6e. The patient with partial response, a >30% decrease in tumor volume (Fig. 6c), was diagnosed in February 2000 and had already undergone eight chemotherapy regimens (Fig. 6d). The patient received treatment for a total of 156 days prior to probable disease progression with small bowel obstruction. There was no radiographic evidence of tumor progression.

DISCUSSION

The nucleus is a defining feature of eukaryotes, separating the cell into nuclear and cytoplasmic components. This physical division provides a unique degree of spatial regulation to protein function. XPO1 one of eight known nuclear export proteins that are required for nuclear:cytoplasmic transport of macromolecules through the nuclear pore complex. Notably, XPO1 is the sole nuclear exporter of a number of key cancer-associated proteins, including p53 and I κ B α (46). While other cancer types are increasingly treated successfully, OvCa mortality rates have remained relatively high over the past 50 years, with a 5-yr survival rate at ~30% for patients diagnosed with Stage 3/4 diseases. Given that chemoresistance represents the major cause for OvCa treatment failure (2), our studies were specifically focused on exploring the efficacy and clinical relevance of XPO1 inhibition in treating platinum-resistant OvCa. We believe our findings support a novel role for the use of XPO1 inhibition in platinum-resistant OvCa.

Our results demonstrate that inhibition of XPO1 by two SINE compounds (KPT-185 and selinexor/KPT-330) was significantly associated with increased tumor killing, regardless of tumor platinum sensitivity or p53 status. Notably, we demonstrated a synergistic effect between KPT-185 and cisplatin in all immortalized and primary patient-derived cell lines tested. Moreover, selinexor and cisplatin co-treatment yielded the greatest overall survival and reductions in tumor size in two OvCa mouse models. Most dramatically, the oral XPO1 inhibitor selinexor was safely tolerated by five OvCa patients and that for the majority (3/5) of these patients, even in the setting of late-stage, heavily pretreated and chemoresistant disease, XPO1 inhibition stabilized

the disease and/or shrank the tumor, with the longest treatment lasting over 1 year. Based upon our findings of drug synergy, combined usage of SINE and platinum agents in future clinical studies may achieve an even greater antitumor effect.

Since nearly 100% of late-stage serous ovarian tumors have defects in p53 (41), it was necessary to define the mechanism through which XPO1 inhibition resulted in cell death in p53-mutated cells. In both SKOV3 and OVCAR3 cell lines, in which p53 is either null or mutated, respectively, XPO1 inhibition resulted in increased nuclear levels of I κ B α with consequent physical interaction with p65 and inhibition of NF- κ B activity. This is consistent with a number of previous findings that have demonstrated that inhibition of NF- κ B activity can induce cell death (43). In general, NF- κ B activity can be regulated through the shuttling of key interacting proteins, most notably I κ B α , between cytoplasm and nucleus (47). NF- κ B signaling is known to be constitutively active (localized to the nucleus) in multiple cancers, including OvCa, and this activation is not necessarily dependent upon intrinsic mutations in NF- κ B (44). NF- κ B's regulator I κ B α , is sequestered in the cytoplasm and/or degraded by the proteasome. Forced retention of I κ B α in the nucleus by SINEs leads to binding of I κ B α to NF- κ B and results in termination of NF- κ B binding to DNA, neutralizing its transcriptional activity. Our findings may be especially relevant in serous OvCa since NF- κ B has been shown to be not only continuously active in OvCa, playing a role in the development and maintenance of OvCa and chemotherapy resistance (48) but NF- κ B activity may be further increased in p53 mutant cells (49). In contrast to this finding, in the two cell lines with wild type p53, A2780 and CP70, XPO1 inhibition resulted in a marked nuclear shift of p53 and activation of its downstream target, ERK1/2. Activation of ERK1/2 generally promotes cell survival but can, under certain conditions (42), and as we have shown in our model system, have pro-apoptotic functions. Thus, SINE can drive both p53-dependent and -independent apoptosis pathways allowing for broad anti-tumor activity.

In addition to XPO1 a number of nuclear transport proteins are also under study as potential therapeutic targets in cancer including KPNA1-6, KPNB1, TNPO, and IPO (50). Driven in part by the current understanding that nuclear-cytoplasmic export is primarily driven by XPO1, a number of potential therapeutics agents targeting XPO1 have been developed and tested and the small molecule SINE have shown the most promise of clinical efficacy and safety (3-6,51). The XPO1 inhibitor KPT-330 (selinexor) is the only compound currently being evaluated in clinical trials in solid tumors and hematological malignancies. Phase I results in 189 patients

with advanced solid tumors was recently reported by members of our group (33). The ovarian cancer patients in that trial are reported herein. These current studies provide an opportunity to examine in depth the mechanisms underlying cell death in a specific cancer type. In this regard it is important to note that in addition to our current study in OvCA, a recent report also examined the effect of KPT-185 in OvCa models (52). Intriguingly, and adding to the concept that SINE may achieve their effectiveness through a number of different pathways, these authors identified eIF5A and IGF2BP1 as playing an important role in KPT-mediated cell death in vitro. Our studies did not highlight these two targets despite the fact that both used the A2780 cell line. The reason for these differences is currently unknown but will be important to pursue to better understand mechanisms of effect and resistance.

The full roster of cancer-relevant cargo transported by XPO1 and the resultant pathway dysregulation(s) caused by inappropriate nuclear-cytoplasmic partitioning resulting from XPO1 overexpression remains unknown. Our studies not only provide the rationale for XPO1 as a therapeutic target in platinum-resistant OvCa, but also demonstrate that XPO1 acts synergistically with cisplatin and highlights that cell death is achieved through both p53-dependent and independent pathways. Thus, future clinical trials targeting platinum-resistant ovarian cancers, which are almost always p53 mutated, could potentially overcome this resistance through combination treatment using both a platinum agent and SINE.

REFERENCES

1. Siegel R, Naishadham D, & Jemal A. Cancer statistics, 2013. *CA Cancer J Clin* 2013; 63:11-30
2. Agarwal R & Kaye SB. Ovarian cancer: strategies for overcoming resistance to chemotherapy. *Nat Rev Cancer* 2003; 3: 502-516.
3. Sekimoto T and Yoneda Y. Intrinsic and extrinsic negative regulators of nuclear protein transport processes. *Genes Cells* 2012; 17: 525-535.
4. Kau TR, Way JC & Silver PA. Nuclear transport and cancer: from mechanism to intervention. *Nat Rev Cancer* 2004; 4: 106-117.
5. Turner JG, Dawson J & Sullivan DM. Nuclear export of proteins and drug resistance in cancer. *Biochem Pharmacol* 2012; 83: 1021-1032.
6. Senapedis WT, Baloglu E & Landesman Y. Clinical translation of nuclear export inhibitors in cancer. *Semin Cancer Biol* 2014; 27: 74-86.
7. Raices M & D'Angelo MA. Nuclear pore complex composition: a new regulator of tissue-specific and developmental functions. *Nat Rev Mol Cell Biol* 2012; 13: 687-699.
8. Chow KH, Factor RE & Ullman KS. The nuclear envelope environment and its cancer connections. *Nat Rev Cancer* 2012; 12: 196-209.

9. van der Watt PJ, Maske CP, Hendricks DT, Parker MI, Denny L, Govender D et al. The Karyopherin proteins, Crm1 and Karyopherin beta1, are overexpressed in cervical cancer and are critical for cancer cell survival and proliferation. *International journal of cancer*. Int J Cancer 2009; 124: 1829-1840.
10. Noske A, Weichert W, Niesporek S, Roske A, Buckendahl AC, Koch I, et al. Expression of the nuclear export protein chromosomal region maintenance/exportin 1/Xpo1 is a prognostic factor in human ovarian cancer. *Cancer* 2008; 112: 1733-1743.
11. Stommel JM, Marchenko ND, Jimenez GS, Moll UM, Hope TJ, Wahl GM, et al. A leucine-rich nuclear export signal in the p53 tetramerization domain: regulation of subcellular localization and p53 activity by NES masking. *EMBO J* 1999; 18: 1660-1672.
12. Nikolaev AY, Li M, Puskas N, Qin J, & Gu W. Parc: a cytoplasmic anchor for p53. *Cell* 2003; 112: 29-40.
13. Garcia JM, Rodriguez R, Silva J, Munoz C, Dominguez G, Silva JM, et al. Intratumoral heterogeneity in microsatellite alterations in BRCA1 and PTEN regions in sporadic colorectal cancer. *Ann Surg Oncol* 2003; 10:876-881.
14. Johnson C, Van Antwerp D. & Hope TJ. An N-terminal nuclear export signal is required for the nucleocytoplasmic shuttling of I κ B α . *EMBO J*1999; 18: 6682-6693.
15. Rodriguez E, Aburjania N, Priedigkeit NM, DiFeo A & Martignetti JA. Nucleo-cytoplasmic localization domains regulate Kruppel-like factor 6 (KLF6) protein stability and tumor suppressor function. *PLoS One* 2010; 5
16. Thakar K, Karaca S, Port SA, Urlaub H & Kehlenbach RH. Identification of CRM1-dependent Nuclear Export Cargos Using Quantitative Mass Spectrometry. *Mol Cell Proteomics* 2013; MCP 12: 664-678.
17. Kudo N, Matsumori N, Taoka H, Fujiwara D, Schreiner EP, Wolff B, et al. Leptomycin B inactivates CRM1/exportin 1 by covalent modification at a cysteine residue in the central conserved region. *Proc Natl Acad Sci USA*1999; 96: 9112-9117.
18. Newlands ES, Rustin GJ & Brampton MH. Phase I trial of elactocin. *Br J Cancer* 1996; 74:648-649.
19. Mutka SC, Yang WQ, Dong SD, Ward SL, Craig DA, Timmermans PB, et al. Identification of nuclear export inhibitors with potent anticancer activity in vivo. *Cancer Res* 2009; 69, 510-517.
20. Gademann, K. Controlling protein transport by small molecules. *Curr Drug Targets* 2011; 12: 1574-1580.
21. Sun Q, Carrasco YP, Hu Y, Guo X, Mirzaei H, Macmillan J, et al. Nuclear export inhibition through covalent conjugation and hydrolysis of Leptomycin B by CRM1. *Proc Natl Acad Sci USA* 2013; 110: 1303-1308.
22. Lapalombella R, Sun Q, Williams K, Tangeman L, Jha S, Zhong Y, et al. Selective inhibitors of nuclear export show that CRM1/XPO1 is a target in chronic lymphocytic leukemia. *Blood* 2012; 120: 4621-4634.
23. Etchin J, Sanda T, Mansour MR, Kentsis A, Montero J, Le BT, et al. KPT-330 inhibitor of CRM1 (XPO1)-mediated nuclear export has selective anti-leukaemic activity in preclinical models of T-cell acute lymphoblastic leukaemia and acute myeloid leukaemia. *Br J Haematol* 2013; 161: 117-127.
24. Inoue H, Kauffman M, Shacham S, Landesman Y, Yang J, Evans CP, et al. CRM1 blockade by selective inhibitors of nuclear export attenuates kidney cancer growth. *J Urol* 2013; 189: 2317-2326.

25. Zhang K, Wang M, Tamayo AT, Shacham S, Kauffman M, Lee J, et al. Novel selective inhibitors of nuclear export CRM1 antagonists for therapy in mantle cell lymphoma. *Exp Hematol* 2013; 41:67-78 e64.
26. Pathria G, Wagner C & Wagner SN. Inhibition of CRM1-mediated nucleocytoplasmic transport: triggering human melanoma cell apoptosis by perturbing multiple cellular pathways *J Invest Dermatol* 2012; 132: 2780-2790
27. Sun H, Hattori N, Chen W, Sun Q, Sudo M, E-ling GJ, et al. KPT-330 has antitumour activity against non-small cell lung cancer. *Br J Cancer*. 2014 Jul 15; 111(2): 281–291.
28. Takahito Miyake, Sunila Pradeep, Sherry Y. Wu, Rajesha Rupaimoole, Behrouz Zand, Yunfei Wen, et al. XPO1/CRM1 inhibition causes antitumor effects by mitochondrial accumulation of eIF5A. *Clinical Cancer Res*, 21:3286-97
29. Liu X, Ory V, Chapman S, Yuan H, Albanese C, Kallakury B, et al. ROCK inhibitor and feeder cells induce the conditional reprogramming of epithelial cells. *The American journal of pathology* 2012; 180: 599-607
30. Evans BR, Mosig RA, Lobl M, Martignetti, CR, Camacho C, Grum-Tokars V, et al. Mutation of membrane type-1 metalloproteinase, MT1-MMP causes the multicentric osteolysis and arthritis disease Winchester Syndrome. *Am J Hum Genet* 2012; 91: 572-576.
31. Chou TC. Drug combination studies and their synergy quantification using the Chou-Talalay method. *Cancer Res* 2010; 70: 440-446.
32. Difeo A, Huang F, Sangodkar J, Terzo, EA, Leake D, Narla G, et al. KLF6-SV1 is a novel antiapoptotic protein that targets the BH3-only protein NOXA for degradation and whose inhibition extends survival in an ovarian cancer model. *Cancer Res* 2009; 69: 4733-4741.
33. Razak A, Mau-Soerensen M, Gabrail NY, Gerecitano JF, Shields AF, Unger TJ , et al. First-in-Class, First-in-Human phase I study of selinexor, a selective inhibitor of nuclear export, in patients with advanced solid tumors. *J clin Oncol*, 2016, epub.
34. Gao J, Aksoy BA, Dogrusoz U, Dresdner G, Gross B, Sumer S O, et al. Integrative analysis of complex cancer genomics and clinical profiles using the cBioPortal. *Sci Signal* 2013; 6: p11
35. Gyorffy B, Lanczky A & Szallasi Z. Implementing an online tool for genome-wide validation of survival-associated biomarkers in ovarian-cancer using microarray data from 1287 patients. *Endocr Relat Cancer* 2012; 19: 197-208.
36. Hacker NF, Berek JS, Lagasse LD, Nieberg RK & Elashoff RM. Primary cytoreductive surgery for epithelial ovarian cancer. *Obstet Gynecol* 1983; 61: 413-420.
37. Harrell FE, Jr, Califf RM, Pryor DB, Lee KL & Rosati RA. Evaluating the yield of medical tests. *JAMA* 1982; 247: 2543-2546
38. Parker RJ, Eastman A, Bostick-Bruton F& Reed E. Acquired cisplatin resistance in human ovarian cancer cells is associated with enhanced repair of cisplatin-DNA lesions and reduced drug accumulation. *J Clin Invest* 1991; 87: 772-777.
39. Hamilton TC, Young, RC, McKoy WM, Grotzinger KR, Green JA, Chu EW, et al. Characterization of a human ovarian carcinoma cell line (NIH:OVCAR-3) with androgen and estrogen receptors. *Cancer Res* 1983; 43: 5379-5389.
40. Ormerod MG, O'Neill C, Robertson D, Kelland LR & Harrap KR. cis-Diamminedichloroplatinum(II)-induced cell death through apoptosis in sensitive and resistant human ovarian carcinoma cell lines. *Cancer Chemother Pharmacol* 1996; 37: 463-471.

41. Cancer Genome Atlas Research, N. Integrated genomic analyses of ovarian carcinoma. *Nature* 2011; 474: 609-615
42. Pearson G, Robinson F, Beers Gibson T, Xu BE, Karandikar M, Berman K, et al. Mitogen-activated protein (MAP) kinase pathways: regulation and physiological functions. *Endocr Rev* 2001; 22:153-183.
43. Karin, M. Nuclear factor-kappaB in cancer development and progression. *Nature* 2006; 441: 431-436.
44. Baud V & Karin M. Is NF-kappaB a good target for cancer therapy? Hopes and pitfalls. *Nat Rev Drug Discov* 2009; 8: 33-40.
45. Weroha SJ, Becker MA, Enderica-Gonzalez S, Harrington SC, Oberg AL, Maurer MJ, et al. Tumorgrafts as in vivo surrogates for women with ovarian cancer. *Clin Cancer Res* 2014; 20: 1288-1297.
46. Xu D, Grishin NV & Chook YM. NESdb: a database of NES-containing CRM1 cargoes. *Mol Biol Cell* 2012; 23: 3673-3676.
47. Birbach A, Gold P, Binder BR, Hofer E, de Martin R, & Schmid JA. Signaling molecules of the NF-kappa B pathway shuttle constitutively between cytoplasm and nucleus. *J Biol Chem* 2002; 277: 10842-10851.
48. Alvero AB. Recent insights into the role of NF-kappaB in ovarian carcinogenesis. *Genome Med.* 2010; 2: 56.
49. Weisz L, Damalas A, Lontos M, Karakaidos P, Fontemaggi G, Maor-Aloni R, et al. Mutant p53 enhances nuclear factor kappaB activation by tumor necrosis factor alpha in cancer cells. *Cancer Res.* 2007; 67; 2396-2401.
50. Mahipal A & Malafa M. Imports and exportins as therapeutic targets in cancer. *Pharmacol Ther*, 2016;164:135-143
51. Tan DS, Bedard PL, Kuruvilla J, Siu LL & Razak AR. Promising SINEs for embargoing nuclear-cytoplasmic export as an anticancer strategy. *Cancer Disco.* 2014;4:527-537
52. Miyake T, Pradeep S, Wu SY, Rupaimoole R, Zand B, Wen Y, et al. XPO1/CRM1 Inhibition Causes Antitumor Effects by Mitochondrial Accumulation of eIF5A. *Clin Cancer Res.* 2015; 21(14): 3286-3297.

FIGURE LEGENDS

Figure 1. XPO1 is highly expressed in human OvCa and expression is associated with worse survival. (a) Kaplan-Meier plots of PFS (left panel) and OS (right panel) and XPO1 expression using the program Kaplan-Meier Plotter⁸. Expression data is interrogated from the GEO and TCGA data sets using only those patients with suboptimal debulking and who received platinum as part of their treatment. (b) XPO1 protein expression across multiple OvCa and non-OvCa cell lines. (c) Representative images of XPO1 IHC staining in an ovarian carcinoma TMA. All samples represented in the TMA are high grade serous ovarian cancer. Left: low (H-score=30) cytoplasmic staining. Right: high (H-score=300) nuclear and cytoplasmic staining. The representative fields shown were viewed at 200× magnification. (d) Kaplan–Meier survival plot based on XPO1 protein expression levels in TMA patient tumor samples.

Figure 2. KPT-185 demonstrates antitumor activity selectively in cancer cell lines regardless of p53 status and acts synergistically with cisplatin. (a) Treatment of the four OvCa cell lines, A2780/CP70 (p53 WT), OVCAR3 (p53 mutated) and SKOV3 (p53 null) and six non-cancerous cell lines with different concentrations of KPT-185 for 72 hours. Cell viability was measured by MTT assay and each IC₅₀ calculated as shown in the table beneath the graph. All experiments were performed in triplicate and repeated three times. Results are shown as SD±SE. (b) KPT-185 treatment for 48 hours of CP70, OVCAR3 and SKOV3 results in apoptosis which can be blocked by the pan-caspase inhibitor Z-VAD and treatment results in (c) increased cleaved PARP (C-PARP), and caspases 3, 8, and 9 (C-caspase 3, 8, and 9). (d) Synergistic effect of combined treatment (blue lines) was demonstrated measuring cell viability following initial treatment with different cisplatin concentrations for 24 hours followed by KPT treatment for an additional 48 hours. Pooled data from all four OvCa cell lines is shown in the left lower panel and data from the individual cell lines, in the right upper panels. (e) Summary of p53 status, cisplatin IC₅₀'s and CI's of tested cell lines. IC₅₀-CDDP: IC₅₀ of cisplatin; IC₅₀-CDDP*: IC₅₀ of cisplatin in combination with KPT; CI: combination index, the numbers show the CI calculated at most close to Fa50 by Calculusyn. WT: Wild Type. HD: Homozygous deletion (f) Patient-derived OvCa cell lines (n=17; PDOvCa-CL) were treated with different concentrations of KPT-185 (red line), cisplatin (CDDP, black line) or combination cisplatin and 500 nM KPT (KPT+CDDP, green line) for 48 hours to test for drug synergy. Pooled data from all samples is shown.

Figure 3. KPT-185-induces nuclear accumulation of active ERK1/2 and is p53-dependent in CP70 cells. (a) Immunofluorescence staining of p53 (left panel, middle) and ERK1/2 (right panel, middle) in KPT-185 treated CP70 cells at 48 hours demonstrates nuclear accumulation of these two proteins. DAPI (blue) was used for nuclear counterstaining. 630x magnification. (b) Western blotting of fractionated lysates for p53 and ERK1/2 from cells treated as in (a) were harvested for cytoplasmic and nuclear extracts. Lamin A/C, nuclear protein loading control; GAPDH, cytosolic protein loading control. Quantification of Western blotting for cytosolic protein (left panel) and nuclear protein (right panel) is shown. *, p<0.05. (c) p53-mediated activation of ERK1/2 can be blocked by PFT-α. CP70 cells treated with KPT, PFT-α, or PFT-α and KPT were harvested and nuclear and cytosolic proteins extracted. Nuclear proteins were probed for p-p53 and p-ERK1/2 (upper panel); cytosolic proteins, Bcl-xL (lower panel). Lamin A/C was used as the nuclear protein loading control, GAPDH, the cytosolic protein loading control. Quantification of Bcl-xL Western blotting is shown in a bar graph to the right of the Western blot. * p<0.05. (d) P53-mediated apoptosis is blocked by PFT as measured by FACS analysis.

Figure 4. KPT-185 induces nuclear accumulation of I κ B α and NF- κ B-p65 with subsequent suppression of NF- κ B-p65 activity in p53 mutant cell lines. (a) Immunofluorescence staining of KPT-treated OVCAR3 and SKOV3 cells for NF- κ B-p65 (second column) and I κ B α (fifth column) reveals nuclear accumulation following KPT treatment. 630 \times magnification. (b) Cells treated as in (a) were harvested and cytoplasmic and nuclear extracts were isolated for Western blotting. Quantification of the nuclear and cytoplasmic bands, lower panel beneath the Westerns, demonstrates nuclear specific accumulation of I κ B α and p65. *, p<0.05. (c) Decreased activity of NF- κ B-p65 following KPT treatment was demonstrated by Western blotting of phospho-p65 and its downstream targets the cytoplasmic anti-apoptosis molecules cIAP1 and cIAP2. Quantification of Western blotting is shown to the right. *, p<0.05. (d) Co-immunoprecipitation of nuclear fractions from control and KPT-treated SKOV3 and OVCAR3 cells to detect protein interaction between I κ B α and p65. Inhibition of I κ B α using siRNA (si-I κ B α) results in (e) increased phospho-p65, and its downstream targets cIAP1 and cIAP2, as demonstrated by Western blotting and (f) decreased apoptosis measured by FACS analysis. scRNA, scrambled siRNA control. Quantification of Western results in (e) is demonstrated to the right of the blot. * p<0.05.

Figure 5. KPT-330 displays active antitumor activity in mouse models of platinum resistant OvCa. (a) Survival curves of CP70 tumor mice treated with different regimens. * KPT versus CDDP, p<0.001, ** Combination of KPT and CDDP versus KPT, p=0.01 (b) IHC staining of p53, Ki-67, and TUNNEL from tumor sections treated as in (a). (c) Upper panel: Tumor growth of PDX mice following KPT-330 treatment. Lower panel: Survival curve of PDX mice following KPT treatment. (d) Representative picture demonstrating *ex vivo* tumor sizes. Arrows indicate the tumors. (e) Tumor growth curve in mice treated with different regimens. Inset highlights the growth curves of KPT-330 treatment mice. At the conclusion of the experiment, tumor tissues were obtained from all mice for *ex vivo* analysis. Tumor histology was consistent with high-grade morphology (Supplementary Fig. 4), and immunohistochemical staining revealed that increased p53 nuclear expression, ki-67 down-regulation, and increased apoptosis was observed only in KPT-330 treated (alone or with cisplatin; Fig. 5b).

Figure 6. Effectiveness of KPT-330 in patients with advanced, heavily pretreated OvCa. (a) Clinical features of patients enrolled in the phase I clinical study and the KPT-330 treatment regimen. (b) The pre-treatment regimens and KPT-330 activity in patients. (c) Abdominal CT image of Patient 043-815 before and after fourth dose of KPT-330. (d) KPT-330-related adverse events occurring at least once in > 2 patients (n=7). Responses were evaluated as per Response Evaluation Criteria in Solid Tumors version 1.1 (RECIST 1.1). (e) Changes in serum CA-125 levels. Patients remained on study on average for 96 days (11- 187 days). The CA-125 reduction correlated with patient response.

Figure 1

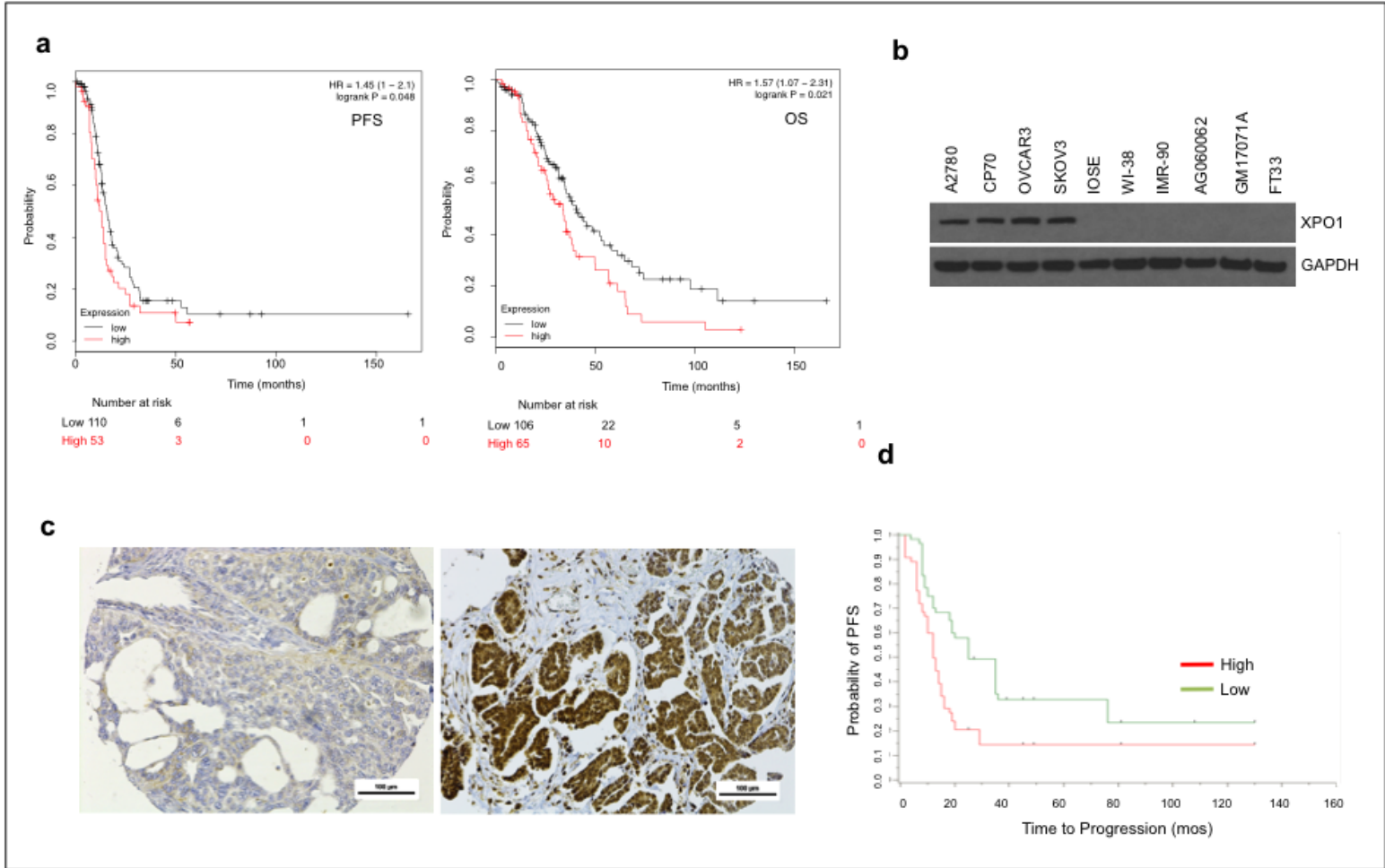


Figure 2

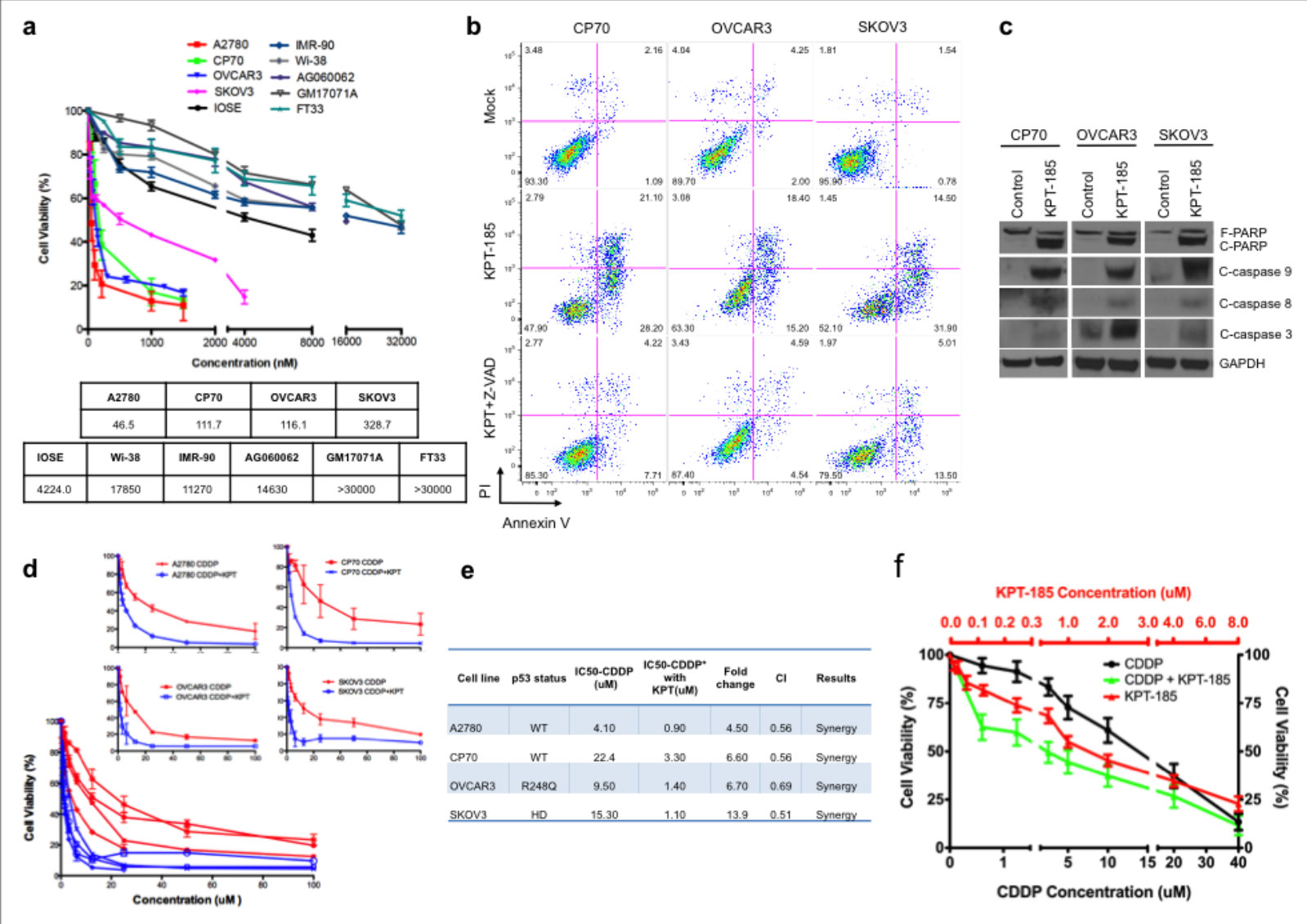


Figure 3

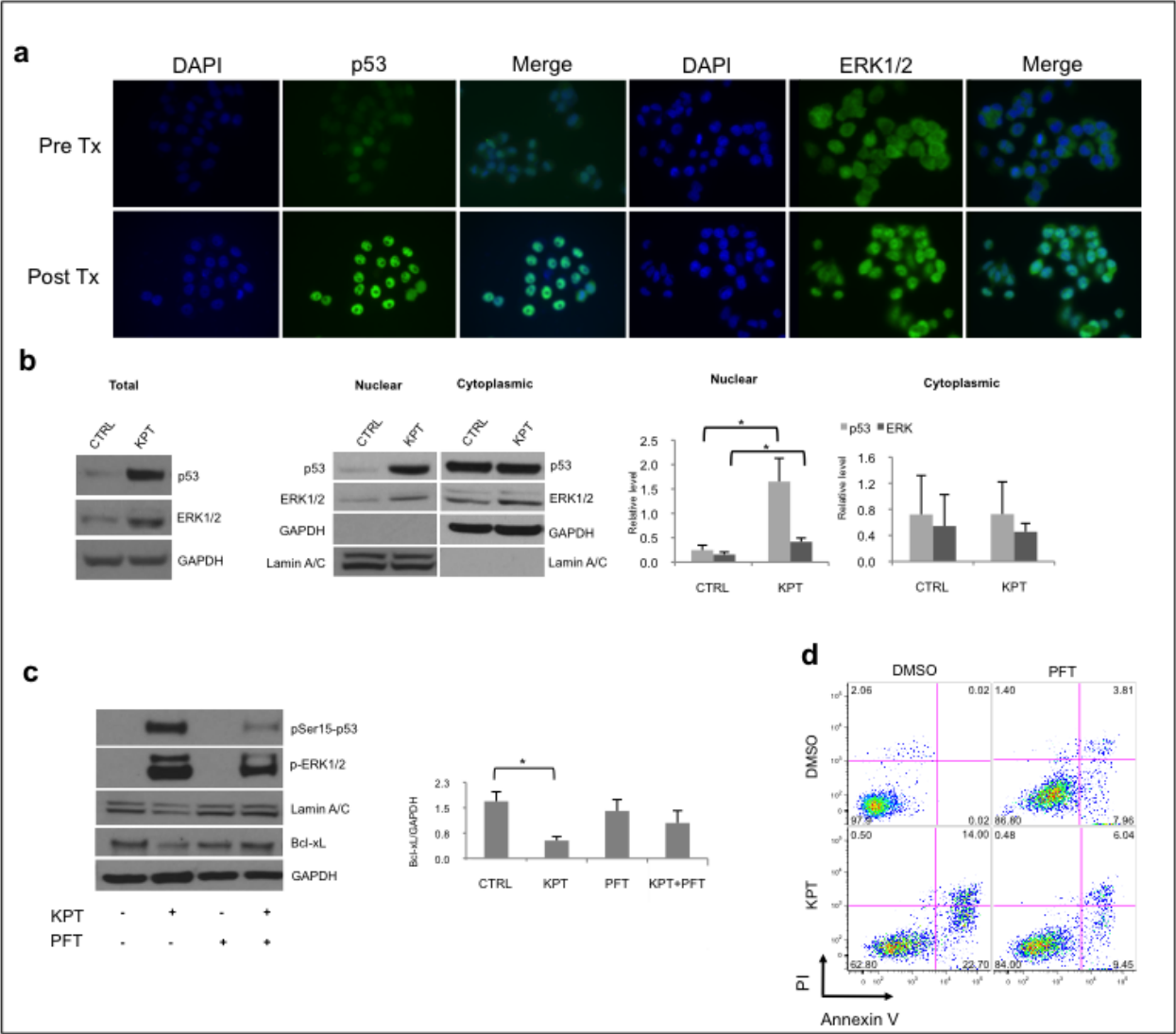


Figure 4

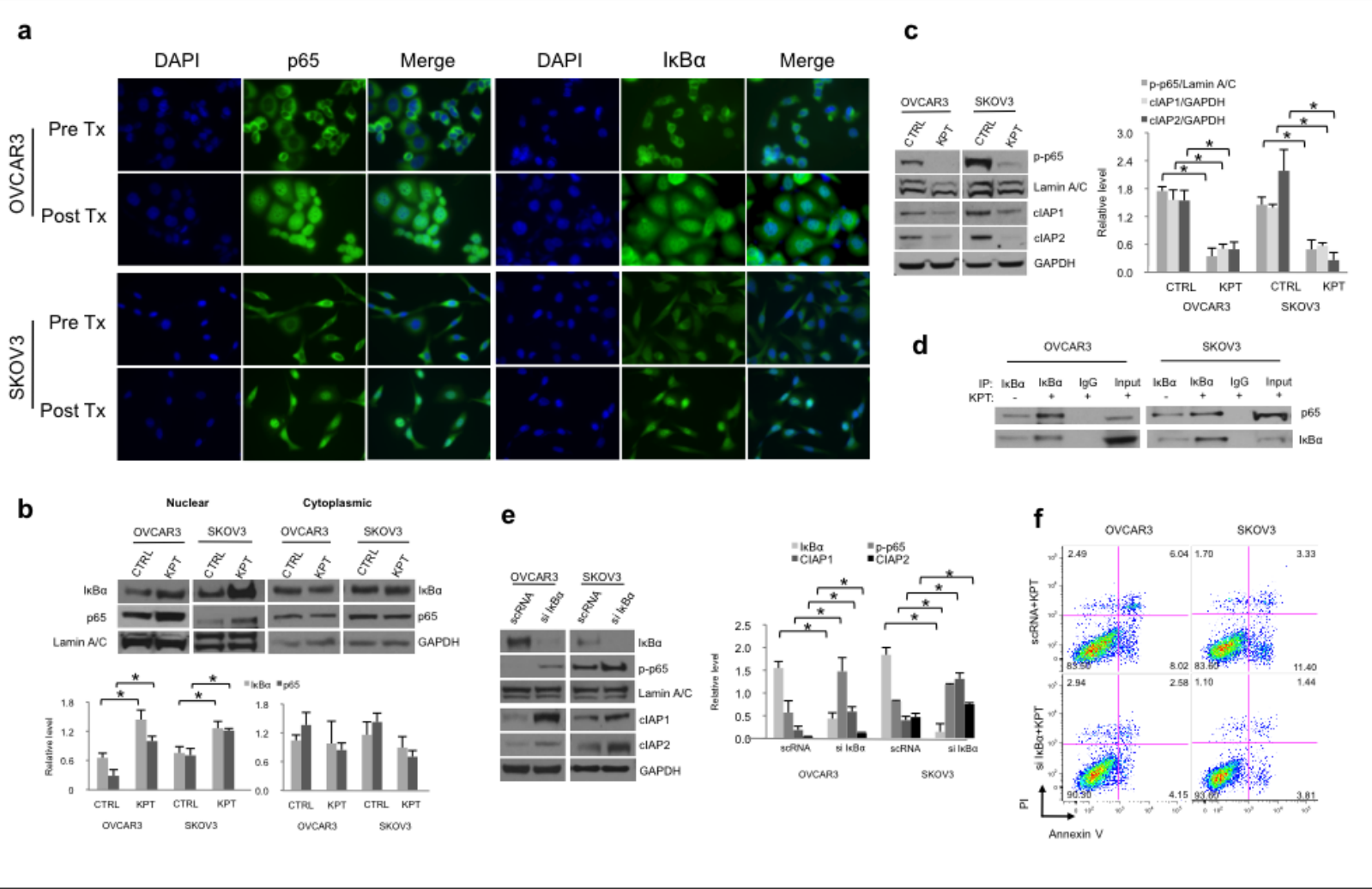


Figure 5

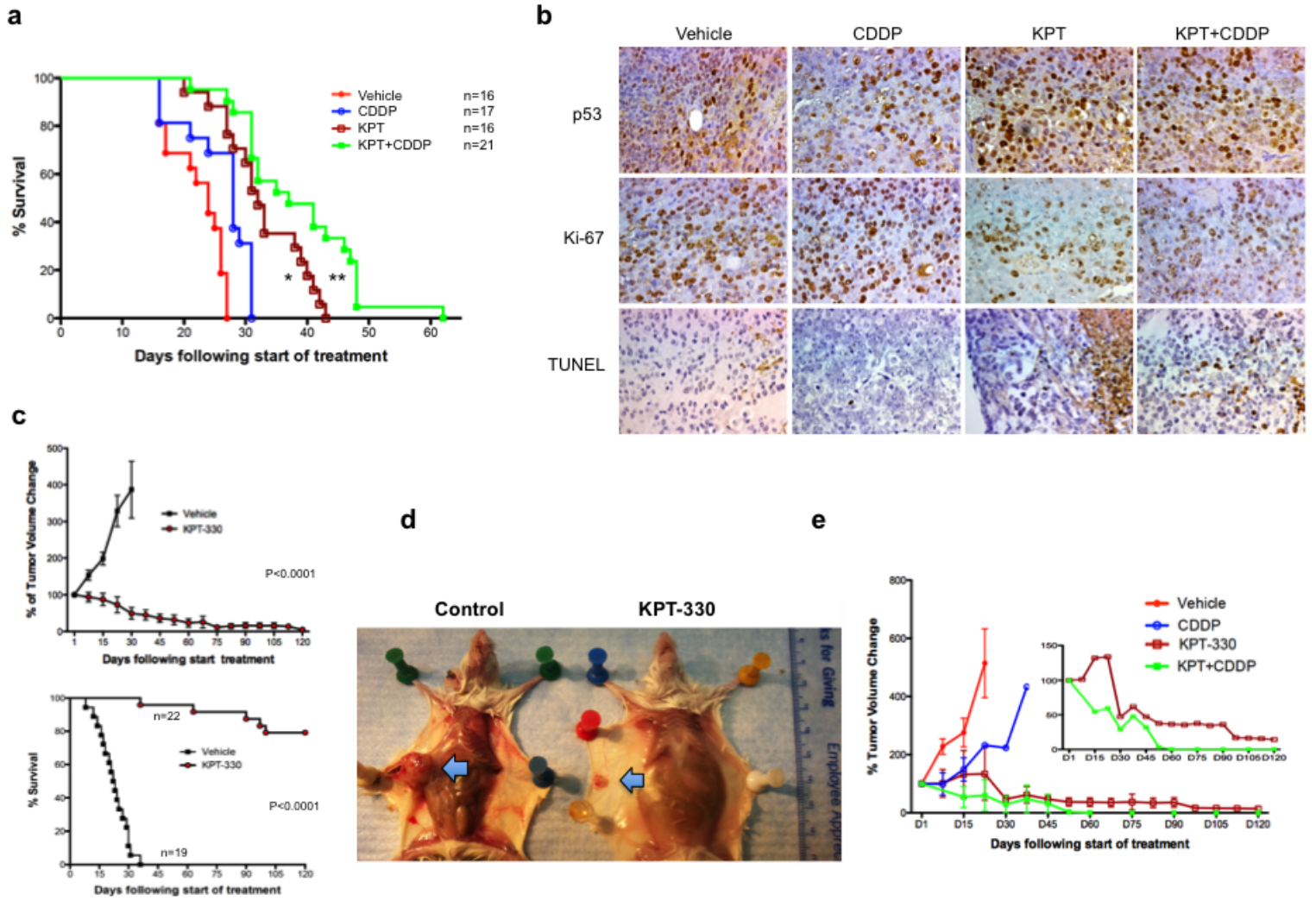


Figure 6

